Quantitative Agarose Gel Electrophoresis of Chromatin: Nucleosome-Dependent Changes in Charge, Shape, and Deformability at Low Ionic Strength†

Terace M. Fletcher, Uma Krishnan,‡ Philip Serwer, and Jeffrey C. Hansen*

Department of Biochemistry, The University of Texas Health Science Center at San Antonio, 7703 Floyd Curl Drive, San Antonio, Texas 78284-7760

Received October 7, 1993; Revised Manuscript Received December 8, 1993®

ABSTRACT: The surface electrical charge density and the deformability of nucleosomal arrays have been characterized by quantitative agarose gel electrophoresis. Monodisperse linear DNA (2.5–3.3 kbp) was reconstituted with histone octamers into either saturated (~1 nucleosome/200-bp DNA) or subsaturated (<1 nucleosome/200-bp DNA) nucleosomal arrays. The electrophoretic mobility (μ) of both nucleosome-free DNA and nucleosomal arrays was determined at low ionic strength in 0.2–3.0% agarose gels. A semilogarithmic plot of μ vs gel concentration was linear for DNA and convex for saturated nucleosomal arrays. By extrapolating the μ to 0% agarose, the magnitude of the gel-free μ of saturated nucleosomal arrays was found to be ~20% lower than that of nucleosome-free DNA molecules. This difference is explained by the net neutralization of ~85 DNA negative charges by each histone octamer. By using an internal standard to measure the effective pore size (P_e) of the agarose gel, the effective radius (R) of DNA and nucleosomal arrays was determined at each agarose concentration. In the more dilute gels ($P_e \geq 400$ nm), the differences between the effective R values of DNA, subsaturated nucleosomal arrays, and saturated nucleosomal arrays are consistent with the differences in their hydrodynamic shapes as measured by analytical velocity centrifugation. However, as P_e decreases, the effective R of both nucleosome-free DNA and subsaturated nucleosomal arrays decreases significantly. This is in contrast to the effective R of saturated nucleosomal arrays, which remains constant at all P_e. The decrease in effective R of the DNA and subsaturated nucleosomal arrays is explained by conformational deformation (i.e., stretching) coupled with reptation during gel electrophoresis [Slater, G. W., Rousseau, J., Nooland, J., Turmel, C., & Lalande, M. (1988) *Biopolymers 27,* 509–524]. These data suggest that the deformability of a nucleosomal array at low ionic strength decreases abruptly as the level of saturation approaches 1 nucleosome per 200-bp DNA.

Eukaryotic DNA is complexed with histone octamers to form nucleosomal arrays (van Holde, 1988; Wolffe, 1992). Nucleosomal arrays exist in several configurations. Those in which nucleosomes are regularly spaced at 200-bp intervals make up the bulk of nuclear chromatin. This configuration is usually associated with transcriptionally inactive gene sequences (Svaren & Chalkley, 1991). Irregular nucleosomal arrays, in which specific regions have been either partly or completely depleted of histones, are often observed near the regulatory regions of either active or potentially active genes (Grunstein, 1990a,b; Svaren & Chalkley, 1991). In some cases, the nucleosomal array is constitutively irregular (Lohr et al., 1987; Fedor et al., 1988), while in other cases a regular array is converted to an irregular array during the process of gene activation (Richard-Foy & Hager, 1987, Carr & Richard-Foy, 1990; Schmid et al., 1992). The presence of nucleosome-free regions within nucleosomal arrays appears to have several effects. At the level of DNA, depletion of nucleosome(s) can lead to enhanced accessibility of trans-acting factors for their DNA binding sites (Workman & Buchman, 1993). Depletion of nucleosomes also promotes unfolding of the nucleosomal array (Hansen & Lohr, 1993), which in turn appears to increase the transcriptional activity of the array (Hansen & Wolffe, 1992).

In considering other potential biological consequences of nucleosome depletion, we have recently become interested in the question of the deformability of nucleosomal arrays. For example, there is in vitro evidence that enhancer-binding proteins and promoter-binding proteins interact over long distances, forming large DNA loops in the process (Su et al., 1991; Li et al., 1991; Mastrangelo et al., 1991). While these studies were performed with naked DNA templates, it has recently been shown that long-range interaction of transcription factors can occur even after the incorporation of DNA into chromatin (Cullen et al., 1993). These results suggest that the chromatin of active genes must be relatively deformable. However, largely due to the absence of suitable analytical methods, the deformability of chromatin has not been carefully investigated.

A technique that potentially can be used to characterize the deformability of nucleosomal arrays is agarose gel electrophoresis. In general, the electrophoretic mobility (μ)[1] of a particle in an agarose gel is dependent on both the gel-free μ (μ_o) and a factor that depends on the particle's size and conformation (Rodbard & Chrambach, 1970; Serwer, 1983; Noolandi, 1992). For rigid spherical particles, it has been demonstrated (Griess et al., 1989) that μ observed during

† This work was supported by NIH Grant GM45916 (to J.C.H.) and NSF Grant DIR 9003695 (to P.S.).

* Corresponding author. Phone: (210) 567-6980. FAX: (210) 567-6595.

‡ Present address: Program in Molecular and Cell Biology, University of Texas at Dallas.

® Abstract published in *Advance ACS Abstracts,* February 1, 1994.

[1] Abbreviations: μ, electrophoretic mobility; μ_o, gel-free μ; P_e, radius of effective gel pore; R, radius, r, moles of histone octamer per mole of 208-bp DNA; N, number of nucleosomes bound per 208-12 DNA molecule; kbp, kilobase pairs; EDTA, ethylenediaminetetraacetate, disodium salt; Tris-HCl, tris(hydroxymethyl)aminomethane hydrochloride; SD, standard deviation.

0006-2960/94/0433-2226$04.50/0

electrophoresis in agarose gels is related to the radius (R) by the equation

$$\mu/\mu'_o = (1 - R/P_e)^2 \quad (1)$$

where μ'_o is μ extrapolated to a gel concentration of 0% agarose, and P_e is the radius of the effective pore at a given agarose gel concentration. By subtracting the μ of electroosmotically driven buffer, the μ'_o can be converted to the μ_o. The $(1 - R/P_e)^2$ term quantifies the sieving by the gel pore network during electrophoresis. After the P_e is determined by use of a spherical standard of known R and μ/μ'_o is measured empirically, the effective R of any particle is determined by solving eq 1 for R. Under conditions in which the effective R approaches P_e, random coils of DNA deform (i.e., become stretched) during gel electrophoresis and move end-first through the gel; this oriented motion is called reptation (Lumpkin et al., 1985; Slater et al., 1987, 1988; Noolandi, 1992). A result of reptation is that the effective R decreases with decreasing P_e (Griess et al., 1990). Thus, the P_e dependence of the effective R provides an assay for the deformability of a nonspherical molecule, such as either DNA or chromatin.

Previous investigations of chromatin behavior in agarose gels have been limited to qualitative studies performed at a single agarose concentration; no attempt has been made to separate the effects of μ_o from the effects of sieving. Simpson et al. (1985) found that in 1% agarose gels, the ratio of the μ of nucleosome-free DNA templates to the μ of length-defined nucleosomal arrays was strongly dependent on the length of the DNA. For ≤600-bp DNA, nucleosomal arrays migrated more slowly than nucleosome-free DNA. However, for ≥1200-bp DNA, the μ of the DNA was unexpectedly similar to the μ of the nucleosomal arrays. In some cases, the nucleosomal arrays actually migrated faster than the DNA. Garcia-Ramirez et al. (1992) recently demonstrated that tryptic removal of the core histone tails caused a marked increase in the magnitude of μ in 1.2% agarose gels. Under these conditions, the trypsinized nucleosomal arrays migrated much more rapidly than the nucleosome-free DNA. To better understand the factors that influence the migration of chromatin molecules through agarose gels, in the present study we have measured both the μ_o and the P_e dependence of the effective R of linear DNA molecules both before and after their reconstitution into regular and irregular nucleosomal arrays.

EXPERIMENTAL PROCEDURES

Materials. Whole chicken blood was obtained from Pel Freeze (Rogers, AR) and used as the source of histone octamers. Chicken erythrocyte histone octamers were purified as described previously (Hansen et al., 1989). The 208-12 DNA template, which consists of 12 tandem 208-bp repeats of *Lytechinus* 5S rDNA (Simpson et al., 1985), was derived from plasmid pPOL 208-12 (Georgel et al., 1993). The pXP10 plasmid contains a single *Xenopus* 5S gene cloned into pUC18 (Wolffe et al., 1986). Both of the plasmids, and the 208-12 DNA, were purified as described (Hansen et al., 1989). The pXP10 DNA was linearized by digestion with *Eco*RI (10 units/μg of DNA) for 60 min at 37 °C. Bacteriophage T3, a roughly spherical DNA bacteriophage that has an R of 30.1 nm, was purified by procedures described previously (Serwer et al., 1983b). Unless otherwise indicated, the agarose used was low-electroosmosis (LE) agarose obtained from Research Organics (Cleveland, OH). Where indicated, Seakem Gold agarose, obtained from FMC Bioproducts (Rockland, ME), was used. All chemicals were of reagent grade. The multigel apparatus described below was obtained from Aquebogue Machine and Repair Shop (Aquebogue, NY).

Reconstitution of Saturated and Subsaturated Nucleosomal Arrays. Nucleosomal arrays were reconstituted from purified histone octamers and DNA, as described by Hansen and Lohr (1993). Histone octamers and either 208-12 DNA or linear pXP10 DNA were mixed and transferred to spectrapor 2 dialysis membranes. The final NaCl and DNA concentrations were 2 M and 100 μg/mL, respectively. The mol of histone octamer/mol of 208-bp DNA (r) ranged from 0.2 to 1.2. The mixtures were subjected to the following stages of dialysis at 4 °C: (a) ≥12 h against 10 mM Tris-HCl/0.25 mM Na_2EDTA (pH 7.8) (20 °C) (TE) buffer containing 1 M NaCl; (b) ≥4 h against TE buffer containing 0.75 M NaCl; and (c) two changes of TE (≥4 h each). After the final dialysis step, 208-12 reconstitutes were subjected to sedimentation velocity analysis in the analytical ultracentrifuge to obtain the integral distribution of sedimentation coefficients. The average number of nucleosomes bound per DNA molecule (N) was determined from the sedimentation coefficient at the boundary midpoint, as described by Hansen and Lohr (1993). Preparations in which ≥50% of the 208-12 DNA molecules were saturated with 12 nucleosomes were achieved at $r = 1.2$. For subsaturated preparations (i.e., $r \leq 1.0$), the distribution around N was ±2 nucleosomes (Hansen & Lohr, 1993).

Sedimentation Velocity. Sedimentation velocity studies were performed in a Beckman XL-A analytical ultracentrifuge equipped with scanner optics. Samples ($A_{260} \cong 0.6$) were sedimented at 18000–28000 rpm using 12-mm double-sector cells and a four-hole Ti60 rotor. The temperature was 20 ± 0.1 °C. The digitized scans were analyzed by the method of van Holde and Weischet (1978) using the XL-A Ultrascan data analysis software program (B. Demeler, Missoula, MT). The van Holde and Weischet analysis graphically removes the contribution of diffusion to the boundary shape and yields the integral distribution of sedimentation coefficients present in the sample [see Hansen and Wolffe (1992) and Hansen and Lohr (1993)]. Each sedimentation coefficient was corrected to $s_{20,w}$, as described previously (Hansen & Lohr, 1993).

Measurement of μ and μ'_o. To determine μ as a function of agarose concentration, electrophoresis through nine gels (running gels), each of a different concentration and all embedded in a single 1.5% agarose frame, was performed at 1 V/cm (Serwer, 1986). Both frame and running gels (the combination is called a multigel) were cast in 40 mM Tris–acetate/1 mM EDTA (pH 7.8) (25 °C) running buffer (TAE). A 10-μL sample containing 0.5–1.0 μg of bacteriophage T3, and 0.6 μg of either DNA or nucleosomal arrays in TE buffer, was loaded in each well. Running buffer was circulated throughout the experiment. Unless otherwise indicated, the temperature was 24 ± 3 °C. Where indicated, the temperature was controlled more accurately (24 ± 0.3 °C) by use of a procedure for Peltier cell-based control of temperature (Serwer & Dunn, 1990). After electrophoresis, DNA was observed by staining with ethidium bromide. Histones subsequently were visualized by staining with Coomassie blue. Photographs of stained gels were digitized (Griess et al., 1992) and measured by use of the software, NIH IMAGE (O'Neill et al., 1989). Values of μ were calculated from the distance (in centimeters) from the well to the front of the band. To obtain μ'_o, the linear region of a semilogarithmic plot of μ vs agarose concentration (Ferguson plot) was extrapolated to a gel concentration of 0% agarose using a standard least-squares linear regression.

Determination of μ_o, R_s, and P_e. To obtain both the μ of electroosmotically driven buffer in LE agarose (μ_E) and the μ_o for bacteriophage T3 (μ_o^{T3}), the μ'_o for T3 ($\mu'_o{}^{T3}$) was determined, by use of Peltier-based temperature control, in both LE agarose and Seakem Gold agarose. For accuracy, running gels for both agarose preparations were cast in the same frame [see Serwer and Hayes (1982)]. Because Seakem Gold agarose has almost no detectable electroosmosis, μ_o^{T3} was assumed to be equal to $\mu'_o{}^{T3}$ in the Seakem Gold agarose: -0.755×10^{-4} cm^2/V·s. To obtain μ_E in LE agarose, the $\mu'_o{}^{T3}$ in Seakem Gold agarose was subtracted from the $\mu'_o{}^{T3}$ in LE agarose. The value of μ_E was 0.102×10^{-4} cm^2/V·s. To obtain the μ_o for either DNA or nucleosomal arrays in LE agarose, bacteriophage T3 was used as an internal standard. After both $\mu'_o{}^{T3}$ and the μ'_o for the particle whose μ_o was to be measured ($\mu'_o{}^{x}$) were determined empirically the following equation was used to obtain $\mu_o{}^{x}$:

$$\mu_o{}^{x} = [(\mu'_o{}^{x})(\mu_o{}^{T3} + \mu_E)/\mu'_o{}^{T3}] - \mu_E \quad (2)$$

The use of bacteriophage T3 as an internal standard for the determination of μ_o eliminated experimental errors that were caused by variations in either mean temperature or mean electrical field during electrophoresis. Without an internal standard, the comparisons of μ_o values made here would not be possible.

The μ and μ'_o of bacteriophage T3, together with its known R (30.1 nm), were used to calculate the P_e of the gels at different agarose concentrations by use of eq 1. The measured μ and μ'_o for both DNA and nucleosomal arrays were then used, together with the P_e determined from the T3 standard in the same multigel, to calculate the effective R of DNA and nucleosomal arrays using eq 1.

RESULTS

In low ionic strength buffers such as TE, nucleosomal arrays adopt an unfolded "beads-on-a-string" structure [see van Holde (1988) for a review]. Saturated 208-12 nucleosomal arrays in TE sediment as a homogeneous ~29S species (Hansen et al., 1989; Garcia-Ramirez et al., 1992). In contrast, 208-12 nucleosomal arrays in 40 mM NaCl form a heterogeneous population of structures, whose sedimentation coefficients range from 32S to 40S (Hansen et al., 1989). The 40S species is a zig-zag-like folded structure (Garcia-Ramirez et al., 1992) that appears to be stabilized by a continuous flow of nucleosome–nucleosome interactions (Yao et al., 1991; Garcia-Ramirez et al., 1992; Hansen & Lohr, 1993). Structures that sediment at <40S are partially unfolded; i.e., only a fraction of the nucleosomes is interacting (Garcia-Ramirez et al., 1992). The TAE running buffer used for the electrophoresis experiments contained 40 mM Tris–acetate/1 mM Na_2EDTA (pH 7.8) (25 °C).

To determine the extent to which the 208-12 nucleosomal arrays were folded in running buffer, we performed boundary sedimentation velocity experiments in TE and TAE buffers. Figure 1 shows the $s_{20,w}$ in TAE divided by the $s_{20,w}$ in TE across the sedimentation coefficient distribution. The vertical profile indicates that there was no significant increase in sedimentation coefficient heterogeneity in TAE. However, the $s_{20,w}$ of the nucleosomal arrays in TAE was ~10% greater than that in TE (32.5S in TAE vs 29.6S in TE at the boundary midpoint). The small but significant increase in $s_{20,w}$ in TAE could reflect either a subtle change in the shape of each nucleosome or a low level of nucleosome–nucleosome interactions. However, the change in $s_{20,w}$ does not approach the 40% increase that occurs upon compaction into the 40S structure. Thus, 208-12 nucleosomal arrays appear to be largely unfolded in TAE running buffer.

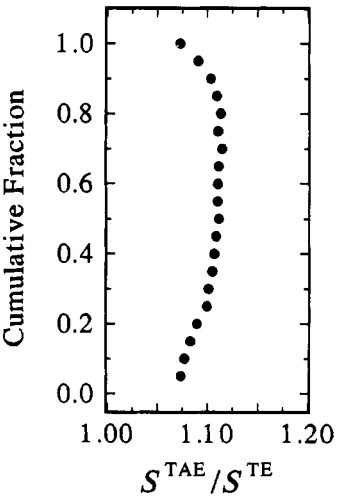

FIGURE 1: Sedimentation velocity analysis of the structure of 208-12 nucleosomal arrays in TAE buffer. A 1.0-mL aliquot of $r = 1.2$ 208-12 nucleosomal arrays (originally in TE buffer) was dialyzed against 1.0 L of TAE buffer for 4 h at 4 °C. Samples of the nucleosomal arrays in either TE or TAE were then sedimented in the Beckman XL-A analytical ultracentrifuge, and the boundaries were analyzed by the method of van Holde and Weischet (1978) to obtain the $s_{20,w}$ distributions, as described under Experimental Procedures. The data are presented as the ratio of the $s_{20,w}$ in TAE buffer relative to the $s_{20,w}$ in TE buffer at each point in the distribution (s^{TAE}/s^{TE}). The $s_{20,w}$'s obtained at the boundary midpoint in TAE and TE were 32.5S and 29.6S, respectively.

Determination of μ. The first step in the determination of both the μ_o and the effective R of nucleosomal arrays and nucleosome-free DNA was to measure the μ as a function of agarose concentration by use of a multigel. After staining with the DNA-specific stain, ethidium, the bands formed by the internal standard bacteriophage T3 (horizontal lines, Figure 2A) were closer to the origin than the bands formed by either the 208-12 DNA (2.5 kbp) or the saturated 208-12 nucleosomal arrays. As expected, both nucleosomal arrays and bacteriophage T3 stained with the protein-specific stain, Coomassie blue; the nucleosome-free DNA did not (Figure 2B).

To determine whether μ was being altered by either reversible particle–particle or particle–gel interactions during electrophoresis, we determined μ as a function of the nucleosomal array concentration. The absence of detectable amounts of these interactions was indicated by the observation that the μ of 208-12 nucleosomal arrays was independent of the amount of sample loaded over at least a 15-fold range (0.36–5.4 g/cm^2 of area at the surface of entry into the gel) (data not shown). To determine whether the histones were dissociating from the 208-12 nucleosomal arrays during electrophoresis, two-dimensional electrophoresis was performed in which nucleosomal arrays and bacteriophage T3 were electrophoresed through a 2% agarose gel at 1 V/cm in both dimensions. If dissociation occurred before electrophoresis, a free DNA band would be present on the line determined by the origin of electrophoresis and the intact bacteriophage T3 band (T3, Figure 3). For example, in the absence of Mg^{2+}, some T3 DNA was released from bacteriophage T3 particles prior to electrophoresis (T3 DNA, Figure 3). If dissociation occurred during electrophoresis, the band(s) would not be on the line. This was observed for a minor fraction of DNA released during electrophoresis from particles of the bacteriophage T3 (T3*, Figure 3). In contrast to the bacteriophage T3 sample, a preparation of 208-12 nucleosomal

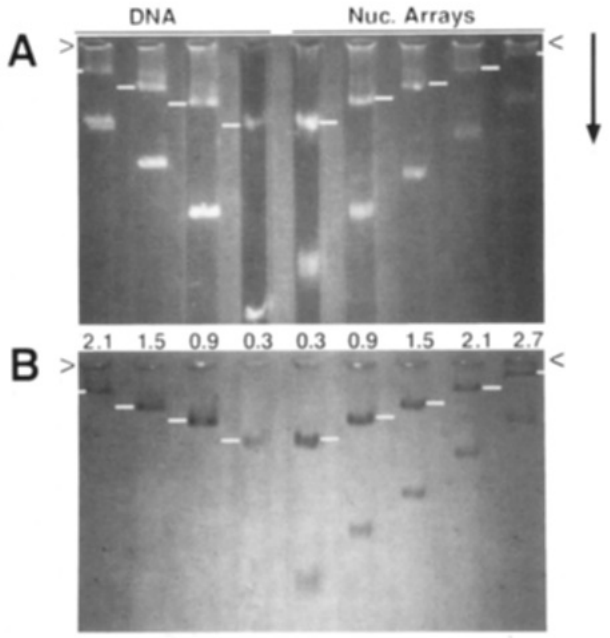

FIGURE 2: Electrophoresis of 208-12 DNA, 208-12 nucleosomal arrays, and bacteriophage T3 in a multigel. The agarose gel concentrations (percentage) are indicated in the figure. Lanes 1–4 contained 208-12 DNA (1.2 μg). Lanes 5–9 contained $r = 1.2$ 208-12 nucleosomal arrays (1.2 μg). Bacteriophage T3 (1 μg), indicated by horizontal lines, was present in all of the lanes. Electrophoresis was performed for 8 h at 1 V/cm. The arrowheads indicate the origins of electrophoresis; the arrow indicates the direction of electrophoresis. (A) The multigel after staining with ethidium bromide. (B) The same multigel after staining with Coomassie blue.

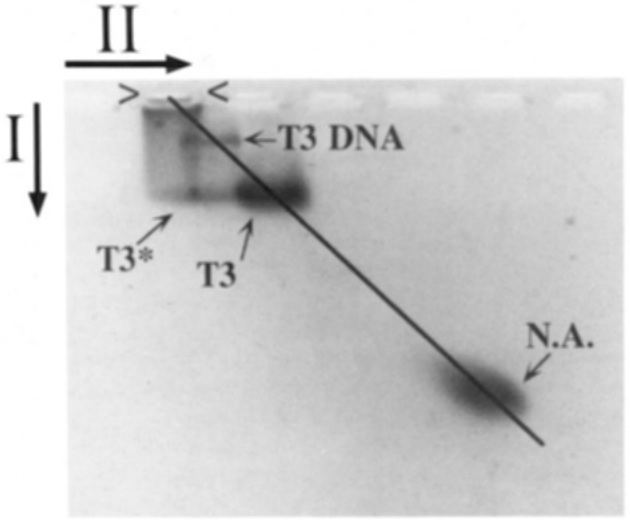

FIGURE 3: Two-dimensional agarose gel electrophoresis of 208-12 nucleosomal arrays and bacteriophage T3. The gel concentration was 2.0%. The arrow pointing down (I) indicates the direction of electrophoresis in the first dimension. The arrow pointing from left to right (II) indicates the direction of electrophoresis in the second dimension. Both dimensions were run at 1 V/cm for 12 h. The temperature was 24 ± 3 °C. The arrowheads indicate the well in which the bacteriophage and nucleosomal array samples were loaded. The other wells were not used in this experiment. The band formed by intact bacteriophage T3 is labeled T3. T3 DNA that was released from a portion of the bacteriophage *prior* to electrophoresis (due to the absence of Mg^{2+} in the running buffer) is labeled T3 DNA. T3 DNA that was released from a portion of the bacteriophage during electrophoresis is labeled T3*. The band formed by a preparation of $r = 1.2$ 208-12 nucleosomal arrays is labeled NA. Approximately 50% of the DNA molecules in this preparation were saturated with 12 nucleosomes, while the remainder of the molecules contained 10–11 nucleosomes.

arrays reconstituted at $r = 1.2$ formed a single band on the line (NA, Figure 3). The staining profile of this band was the same for ethidium as it was for Coomassie blue. Thus, no dissociation of histones was detected.

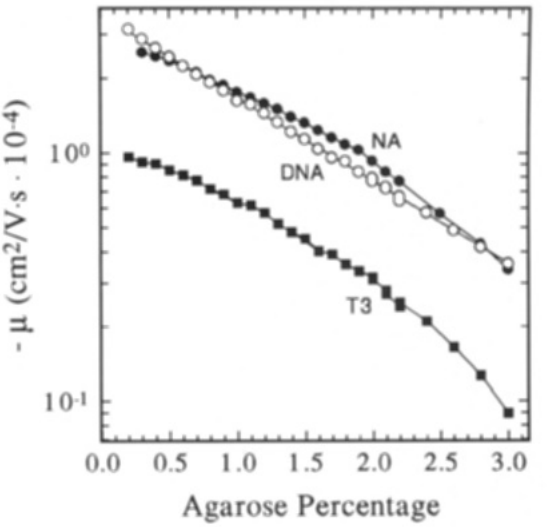

FIGURE 4: Ferguson plots of saturated 208-12 nucleosomal arrays, 208-12 DNA, and bacteriophage T3. The μ values of $r = 1.2$ 208-12 nucleosomal arrays (●), 208-12 DNA (○), and bacteriophage T3 (■) were determined as described under Experimental Procedures. Each Ferguson plot was generated from four partially overlapping multigels, whose agarose percentages ranged over 0.2–0.9%, 1.0–1.5%, 1.3–2.2%, and 2.0–3.0%, respectively. T3, DNA, and NA refer to bacteriophage T3, 208-12 DNA, and $r = 1.2$ 208-12 nucleosomal arrays, respectively.

Ferguson Plots. Ferguson plots of nucleosome-free 208-12 DNA, saturated 208-12 nucleosomal arrays, and bacteriophage T3 are shown in Figure 4. Each plot covered the range of 0.2–3.0% agarose and was constructed from data obtained from multigels with partially overlapping agarose percentages. Consistent with previous results (Serwer et al., 1983a), the Ferguson plot of bacteriophage T3 was convex (i.e., the magnitude of the slope increased as the agarose concentration increased). The μ's of both the nucleosome-free 208-12 DNA and the saturated 208-12 nucleosomal arrays were very similar at all agarose concentrations. However, the shapes of the Ferguson plots of the DNA and nucleosomal arrays were noticeably different. The Ferguson plot of 208-12 DNA was linear, as observed previously for similarly sized DNA when a similar electrical field was used (Serwer, 1980; Stellwagen, 1985). In contrast, the Ferguson plot of saturated 208-12 nucleosomal arrays had a convex curvature, like that of T3 and other rigid spherical particles (Serwer et al., 1983a; Gottlieb, 1985). It should be noted that the saturated 208-12 nucleosomal arrays migrated more slowly than the nucleosome-free DNA in ≤0.5% agarose, but more rapidly than the DNA in 1.0–2.5% agarose (Figure 4). A more rapid migration of saturated nucleosomal arrays in 1.0% agarose was first demonstrated by Simpson et al. (1985).

To better understand the basis of the difference between the electrophoretic behavior of saturated nucleosomal arrays and that of nucleosome-free DNA in Figure 4, we next determined the contributions of μ_o and effective R to the observed μ of 208-12 DNA and 208-12 nucleosomal arrays.

Determination of μ_o. The μ_o of DNA was found to be (2.42 ± 0.02) × 10^{-4} $cm^2/V{\cdot}s$ (Figure 5). This agreed well with previous estimates of the μ_o of other DNA fragments (Olivera et al., 1964; Serwer & Allen, 1984; Stellwagen, 1985; Slater et al., 1988; Orbán et al., 1993). The μ_o of saturated 208-12 nucleosomal arrays was (1.95 ± 0.03) × 10^{-4} $cm^2/V{\cdot}s$, a 20% reduction compared to that of the nucleosome-free DNA. The μ_o decreased linearly with increasing number of nucleosomes/DNA molecule (Figure 5). Thus, binding of a chicken

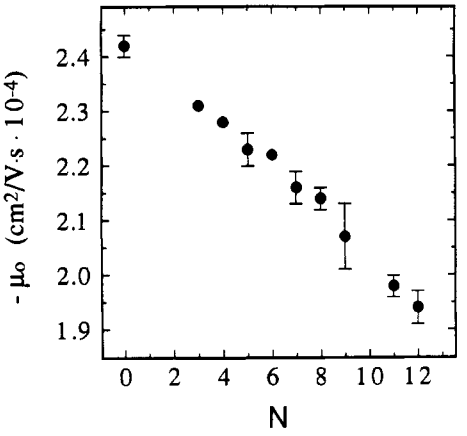

FIGURE 5: Nucleosome-dependent changes in the μ_o of 208-12 DNA. Data were acquired from multigels whose agarose percentages ranged from 0.2 to 1.0%. Procedures are described under Experimental Procedures. The average number of nucleosomes bound per 208-12 DNA molecule, N, was determined from sedimentation velocity analysis as described by Hansen and Lohr (1993). Data points without error bars represent single determinations. Data points with error bars represent the mean ±1 SD of 2–3 determinations.

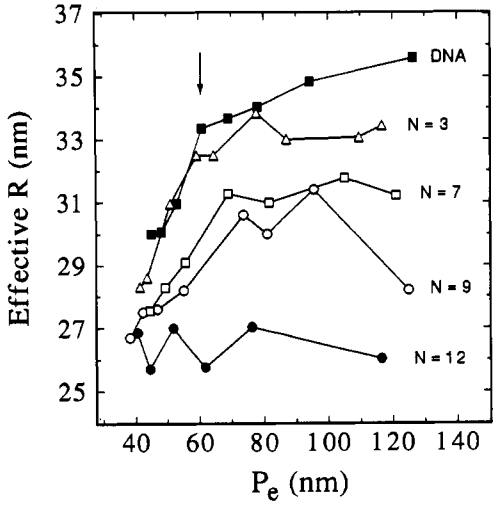

FIGURE 6: Effective R values of 208-12 DNA and 208-12 nucleosomal arrays as a function of P_e. Data were acquired from multigels whose agarose percentages ranged from 0.9 to 3.0%. Procedures are described under Experimental Procedures. Each multigel contained bacteriophage T3 and either 208-12 DNA (■) or N = 3 (△), N = 7 (□), N = 9 (○), or N = 12 (●) 208-12 nucleosomal arrays.

erythrocyte histone octamer to 208 bp of DNA lowers the μ_o of the DNA by 20%.

Effective R as a Function of P_e. The $(1 - R/P_e)^2$ term of eq 1 quantifies the sieving of spheres (Griess et al., 1989). For nonspherical molecules, eq 1 is used to calculate an effective R. In the case of rod-shaped particles, the effective R previously has been shown to best approximate the radius of a sphere that has a surface area equal to the surface area of the rod (Griess et al., 1990). The effective R of saturated 208-12 nucleosomal arrays was an invariant 26–27 nm when determined in gels that had P_e values of 40–120 nm (~0.9–3% agarose) (Figure 6). In addition, the effective R of saturated 208-12 nucleosomal arrays remained unchanged even in very dilute gels, i.e., at $P_e \cong 400$ nm (Table 1). In contrast, the effective R of the 208-12 DNA was strongly P_e-dependent. At $P_e \geq 200$ nm, 208-12 DNA had a constant effective R of about 45 nm (Table 1; data not shown). However, as the P_e was decreased to 120 nm, the effective R of the 208-12 DNA decreased to a value of ~35 nm (Figure 6). At $P_e \cong 60$ nm, the effective R of the 208-12 DNA decreased more sharply (arrow, Figure 6). By $P_e \cong 40$ nm, the effective R of the DNA was 30 nm.

Table 1: Frictional Properties and Effective R at Very High P_e

template	size	f/f_o[a]	effective $R^{0.3\%}$ [b]
208-12 DNA	2512		45 ± 2[c]
pXP10 DNA	3300		55 ± 2
208-12 nuc arrays[d]		3.8	28 ± 1
pXP10 nuc arrays[d]		4.6	34 ± 1

[a] Frictional coefficients were calculated for an unhydrated molecule. [b] The average P_e obtained at 0.3% agarose was 387 ± 14 nm (mean ± SE, n = 15). [c] These values represent a single determination at 0.3% agarose. The error was estimated from the error in the determination of P_e at this agarose concentration (see footnote *b*). [d] Nucleosomal arrays were reconstituted at r = 1.2.

The P_e dependence of the effective R of subsaturated 208-12 nucleosomal arrays resembled that of the histone-free DNA. At $P_e \geq 200$ nm, the effective R of 208-12 DNA molecules containing an average of 3, 5, 7, and 9 nucleosomes was 49.1 ± 2.9, 40.0 ± 1.7, 35.1 ± 2.5, and 33.0 ± 3.4 nm, respectively[2] (data not shown). Like that of the histone-free DNA, the effective R of the subsaturated nucleosomal arrays decreased as the P_e was lowered to 60 nm and decreased sharply at P_e <60 nm (Figure 6). By P_e = 40 nm, the effective R of all of the subsaturated nucleosomal arrays had converged at ~27 nm. The molecular basis for these results will be discussed in more detail. However, it is clear that, for the 208-12 DNA and $N \leq 9$ subsaturated nucleosomal arrays, the effective R at $P_e \geq 200$ nm is significantly larger than the effective R at P_e = 40 nm. This is in contrast to the saturated 208-12 nucleosomal arrays, which have the same effective R at all P_e values.

Electrophoretic Properties of Linear pXP10 DNA and Nucleosomal Arrays. To determine whether the electrophoretic behavior of nucleosomal arrays was dependent on either size or nonuniform nucleosome positioning, we repeated the experiments of Figures 4–6 using linearized pXP10 DNA and linear pXP10 nucleosomal arrays. The pXP10 DNA is ~30% longer than the 208-12 DNA and is >90% random sequence (Wolffe et al., 1986). Nonetheless, pXP10 reconstitutes were similar to 208-12 reconstitutes in that the log $s_{20,w}$ increased linearly as a function of increasing r (data not shown). This indicates that, at any given r, the average density of nucleosomes on the pXP10 DNA is the same as the average density on the 208-12 DNA; i.e., an average of 0.5 and 1 nucleosome per 200 bp of DNA is achieved at r = 0.6 and 1.2, respectively [see Hansen and Lohr (1993)]. However, light micrococcal nuclease digestion of pXP10 nucleosomal arrays yielded a smear of high molecular weight digestion products on 1.0% agarose gels (compared to the defined ladder of bands seen with 208-12 nucleosomal arrays), as well as shorter DNA bands corresponding to close-packed dimers and trimers (data not shown). Thus, unlike those on the 208-12 DNA, the nucleosomes on the pXP10 DNA were not positioned uniformly.

Despite the differences in size and nucleosome positioning, the shapes of the Ferguson plots of linear pXP10 DNA and r = 1.2 pXP10 nucleosomal arrays (Figure 7) were quite similar to those of the 208-12 DNA and r = 1.2 (saturated) 208-12 arrays (Figure 4). The pXP10 DNA did, however, exhibit a very slightly concave curvature, as observed previously for DNA of this size (Serwer, 1980; Stellwagen, 1985). The μ_o's of the pXP10 DNA and r = 1.2 pXP10 nucleosomal arrays (Figure 7) were the same as those of the 208-12 DNA and

[2] Each value represents the mean standard deviation of four determinations of the effective R at P_e values ranging from 200 to 400 nm.

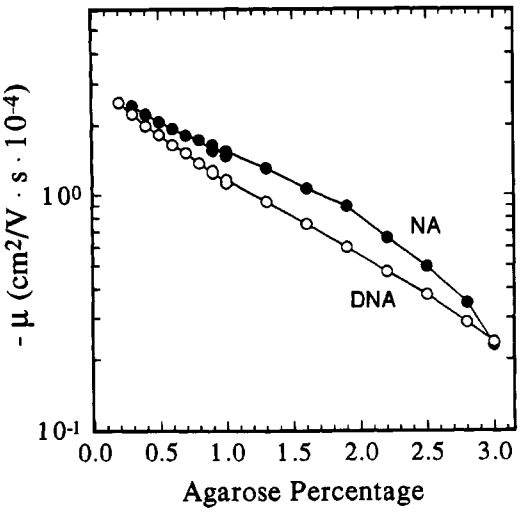

FIGURE 7: Ferguson plots of linear $r = 1.2$ pXP10 nucleosomal arrays (●) and linear pXP10 DNA (○). Each Ferguson plot was generated from two partially overlapping multigels whose agarose percentages ranged over 0.2–1.0% and 0.9–3.0%, respectively. DNA and NA refer to pXP10 DNA and $r = 1.2$ pXP10 nucleosomal arrays, respectively. The μ_o's determined from extrapolation of the linear regions of these Ferguson plots to 0% agarose were $(2.4 \pm 0.1) \times 10^{-4}$ cm²/V·s for the pXP10 DNA and $(1.92 \pm 0.16) \times 10^{-4}$ cm²/V·s for the $r = 1.2$ pXP10 nucleosomal arrays.

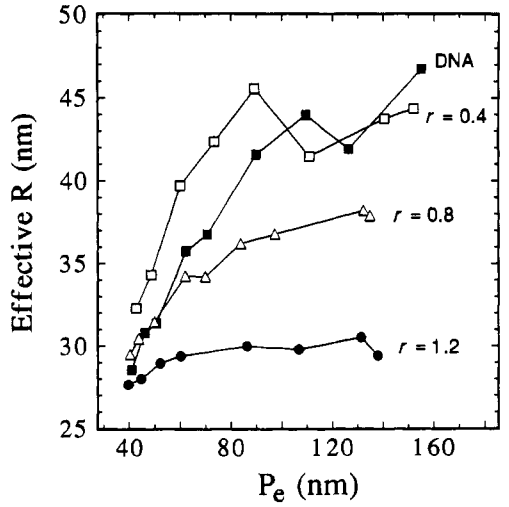

FIGURE 8: Effective R of linear pXP10 DNA and linear pXP10 nucleosomal arrays as a function of P_e. Data were acquired from multigels whose agarose concentrations ranged from 0.9 to 3.0%. Procedures are described under Experimental Procedures. Each multigel contained bacteriophage T3 and either linear pXP10 DNA (■) or linear pXP10 nucleosomal arrays reconstituted at $r = 0.4$ (□), $r = 0.8$ (△), or $r = 1.2$ (●).

saturated 208-12 nucleosomal arrays, as should be the case. Furthermore, the values of μ_o for $r = 0.2$, 0.4, and 0.8 pXP10 nucleosomal arrays were indistinguishable from those of the 208-12 arrays reconstituted at the same r (data not shown). This result would be expected if the μ_o was influenced exclusively by surface charge properties, and not by the particle size and shape. The P_e dependence of the effective R of pXP10 DNA and subsaturated pXP10 nucleosomal arrays also was qualitatively similar to that observed for the 208-12 system (Figure 8). The effective R's of pXP10 DNA and underloaded $r = 0.4$ and 0.8 pXP10 nucleosomal arrays decreased significantly as the P_e was reduced from 120 to 40 nm, while the effective R of highly loaded $r = 1.2$ pXP10 nucleosomal arrays showed comparatively little change over the same P_e range (Figure 8). Given that many of the nucleosomes on the pXP10 DNA were close packed, the small but systematic decrease in the effective R of the $r = 1.2$ pXP10 nucleosomal arrays at P_e <60 nm (Figure 8) may reflect the presence of stretches of nucleosome-free DNA that are longer than those found on the equivalently loaded 208-12 arrays. Finally, as with the 208-12 system, the effective R of pXP10 nucleosomal arrays decreased with increasing degrees of nucleosome loading at $P_e \geq 80$ nm, but not at $P_e = 40$ nm.

DISCUSSION

Surface Electrical Charge of Nucleosomal Arrays. The magnitude of the μ_o of saturated 208-12 nucleosomal arrays was 20% less than that of the 208-12 DNA (Figure 5). The μ_o of a macromolecule, in principle, is proportional to the average electrical surface charge density and is independent of the size of the macromolecule (Shaw, 1969). In agreement, the μ_o of saturated ($r = 1.2$) 208-12 nucleosomal arrays was the same as that of the $r = 1.2$ pXP10 nucleosomal arrays, even though the f/f_o was significantly larger for the pXP10 nucleosomal arrays than it was for the 208-12 nucleosomal arrays (Table 1). Thus, the difference between the μ_o of DNA and the μ_o of nucleosomal arrays appears to result from charge neutralization by the bound histone octamers. A saturated 208-12 nucleosomal array has 1 histone octamer/208 bp of DNA. Assuming a DNA charge of –416 (208 bp × –2), our results predict that each histone octamer contributes ~85 positive charges to the nucleosome *surface*. Similarly, Orbán et al. (1993) recently reported that the μ_o of a nucleosome core particle is ~35% less than the μ_o of nucleosomal DNA, which corresponds to the contribution of ~100 positive charges by the histone octamer. These numbers are reasonable considering that there are ~140 total positive charges in the core histones of the histone octamer, ~100 of which are found in the solvent-exposed histone tails (van Holde, 1988). At least part of the reduction in the net negative surface charge of nucleosomal arrays results from interaction of the core histones with both the nucleosomal DNA and linker DNA regions (Bavykin et al., 1990; Pruss & Wolffe, 1993).

Interpretation of the Sieving of Saturated Nucleosomal Arrays. Because the effective R of saturated 208-12 nucleosomal arrays was independent of P_e, the observed sieving was indistinguishable from the sieving of a spherical particle. This quantitative result is an expression of the qualitative observation of a convex shape for the Ferguson plots of both saturated nucleosomal arrays and bacteriophage T3 (Figures 4 and 7). Although a spherical 55S conformation of a saturated 208-12 nucleosomal array has been observed upon folding in divalent salts (Hansen & Wolffe, 1992), in low-salt TAE running buffer a saturated 208-12 nucleosomal array sediments at 32.5S (Figure 1). A 32.5S sedimentation coefficient is close to that expected for an extended beads-on-a-string type of conformation [see Hansen et al. (1989); Garcia-Ramirez et al., 1992]. Evidence for an extended structure of saturated nucleosomal arrays in low-salt conditions also has been obtained from both electron microscopy (Garcia-Ramirez et al., 1992) and atomic force microscopy (Allen et al., 1993). We therefore conclude that the shape of a saturated 208-12 nucleosomal array in running buffer most closely resembles that of a rod (or a very elongated prolate ellipsoid).

In this respect, Griess et al. (1990) showed that the sieving of a rod is indistinguishable from the sieving of a sphere for P_e values greater than a critical value that is one-half the length of a stiff rod, but smaller if the rod is flexible. For P_e greater than the critical P_e, the characteristic of a rod that best described its sieving was its surface area. If we assume

11 internucleosomal DNA regions of 43 bp[3] and 12 nucleosomes (11 nm in diameter) per 208-12 nucleosomal array, the length of an extended 208-12 nucleosomal array is ~300 nm. The surface area of a rod-shaped envelope having the dimensions 11 × 300 nm is $\sim 10.4 \times 10^3$ nm^2. The surface area calculated from the observed effective R of a saturated 208-12 nucleosomal array (27 ± 1.5 nm) is $(9.2 \pm 0.5) \times 10^3$ nm^2, in close agreement with that predicted for a rodlike conformation. The length of a 208-12 nucleosomal array is 3 times greater than the diameter of the smallest gel pore used in these studies, which is long enough to cause a decrease in effective R at the lower P_e values if the nucleosomal arrays are rigid. Thus, we propose that saturated 208-12 nucleosomal arrays in low-salt buffer are sufficiently flexible to prevent a decrease in effective R, at least for the P_e values used here.

Sieving Mechanism of Nucleosome-Free DNA. In contrast to saturated nucleosomal arrays, the nucleosome-free 208-12 and pXP10 DNA molecules are expected to be random coils in solution. That is, assuming a persistence length of 50 nm (Borochov et al., 1981), the 208-12 and pXP10 DNAs are 17 and 22 persistence lengths long, respectively. Thus, the envelope that determines sieving should be the envelope of a random coil, not the surface area of the envelope of the DNA double helix. In agreement, the surface area of the envelope of the DNA double helix for 208-12 DNA was 5.4×10^4 nm^2, which is 3–5 times greater than the surface area calculated from the effective R of 208-12 DNA at $P_e \cong 400$ and 40 nm, respectively.

Unlike the saturated nucleosomal arrays, the nucleosome-free 208-12 and linear pXP10 DNAs had effective R's that decreased as P_e decreased (Figures 6 and 8). This is the quantitative expression of Ferguson plots more linear for nucleosome-free DNA than those for either saturated nucleosomal arrays or bacteriophage T3 (Figures 4 and 7). Similar behavior, as judged from the shape of the Ferguson plots, has been observed previously for longer DNA [see Stellwagen (1987) for a review]. In these earlier studies, linear or slightly convex-shaped Ferguson plots were attributed to both deformation (i.e., stretching) and orientation (i.e., reptation) of the DNA random coil as the P_e was reduced (Serwer & Allen, 1984). In more recent studies, Slater et al. (1988) have found that, when the P_e is greater than the diameter of the DNA random coil, the DNA molecule migrates from pore to pore in a random walk fashion and without significant deformation of its coiled shape. This has been called the Ogston mechanism of sieving (Slater et al., 1988; Noolandi, 1992). As the diameter of the DNA coil more closely approaches that of the gel pore, the DNA molecule remains largely undeformed, but becomes less capable of lateral movement. This has been termed reptation without stretching. The most extreme mode of sieving occurs under conditions where the gel pore diameter is much smaller than the diameter of the DNA coil. This leads to severe deformation (stretching) and reptation of the DNA molecule (Slater et al., 1988; Noolandi, 1992). Under these conditions, the μ of longer DNA fragments becomes independent of size (McDonnell et al., 1977; Fangman, 1978; Slater et al., 1988). The behavior of the two DNA molecules used in our studies agrees with this scheme. At $P_e \cong 400$ nm, the effective R of the nucleosome-free pXP10 DNA was 22% larger than the effective R of the nucleosome-free 208-12 DNA (Table 1), consistent with the longer pXP10 DNA forming a larger random coil. However, at $P_e = 40$ nm, both the μ and the effective R of the 208-12 and pXP10 DNA molecules were identical (compare Figures 6 and 8), indicating that under these conditions both of the nucleosome-free DNA molecules were reptating and highly stretched.

Interpretation of the Sieving of Subsaturated Nucleosomal Arrays. Like that of the nucleosome-free DNA molecules, the effective R of subsaturated 208-12 nucleosomal arrays containing ≤9 nucleosomes per DNA molecule decreased sharply as the P_e was decreased from 60 to 40 nm (Figure 6). The same behavior was observed for pXP10 nucleosomal arrays that were reconstituted at subsaturating values of r (Figure 8). The decrease in effective R of subsaturated nucleosomal arrays has at least two possible explanations. First, in the region of the missing nucleosome(s), subsaturated nucleosomal arrays also may undergo P_e-dependent conformational changes (i.e., stretching and reptation) that do not occur in the saturated nucleosomal arrays. Alternatively, a decrease in effective R may occur simply because a subsaturated nucleosomal array is longer than a saturated nucleosomal array. For example, loss of 2–3 nucleosomes from a saturated 208-12 nucleosomal array would increase its total extended length by 75–100 nm. We feel that the latter explanation is unlikely for the following reason. An $r = 1.2$ pXP10 nucleosomal array is approximately the same length as an $N = 9$ subsaturated 208-12 nucleosomal array, yet the $r = 1.2$ pXP10 nucleosomal array does not undergo a sharp decrease in effective R at $P_e < 60$ nm. Therefore, the favored explanation is that reptation and stretching of nucleosome-free regions of subsaturated nucleosomal arrays occur.

Further support for the reptation and stretching of subsaturated nucleosomal arrays comes from a comparison of the effective R of the differently loaded 208-12 nucleosomal arrays above and below $P_e = 60$ nm. At $P_e > 60$ nm, the effective R of $N = 3$ nucleosomal arrays is larger than the effective R of $N = 9$ nucleosomal arrays (Figure 6). This is consistent with the fact that the $N = 3$ nucleosomal arrays are longer than the $N = 9$ nucleosomal arrays, and probably more coillike, at higher P_e. However, by $P_e = 40$ nm, the effective R's of both $N = 3$ and $N = 9$ nucleosomal arrays had become reduced to the same value (Figure 6). Thus, like the different-sized DNA molecules, the differently loaded subsaturated nucleosomal arrays behave at lower P_e as if they are reptating and stretching.

Biological Relevance. The observation that only a few nucleosome-free regions are sufficient to dramatically increase the deformability of an otherwise regularly spaced nucleosomal array may have ramifications for eukaryotic transcription mechanisms. There is a significant body of in vitro evidence indicating that transcription factors bound at widely separated sites on a naked DNA molecule interact with one another in the process forming DNA "loops" (Su et al., 1991; Li et al., 1991; Mastrangelo et al., 1991). However, active genes in vivo are not present as naked DNA, but are packaged into nucleosomal arrays (Grunstein, 1990a,b; Svaren & Chalkley, 1991; Wolffe, 1992). Thus, if long-range protein–protein interactions take place in vivo, they must occur within the context of chromatin. This point recently has been emphasized by Cullen et al. (1993), who showed that in vivo estrogen-induced changes in chromatin structure facilitate long-range enhancer–promoter interactions within the regulatory region of the prolactin gene. In this system, estrogen disrupts nucleosomal structures at the promoter, as evidenced by increased nuclease hypersensitivity (Seyfred & Gorski, 1990). However, the DNA between the enhancer and promoter remains in nucleosomal arrays (Seyfred & Gorski, 1990).

[3] For this calculation, we assumed that two complete turns of DNA interact with the histone octamer in the extended beads-on-a-string structure.

In our studies, we have shown that the deformability of a nucleosomal array is significantly increased by the depletion of as few as one or two nucleosomes over a 1–2-kbp region of DNA. Thus, the increased enhancer–promoter interactions observed by Cullen et al. (1993) may result from an increased deformability of the prolactin gene chromatin after disruption of the nucleosomal structures near the promoter by estrogen treatment. Taken together, these results support the notion that the histone depletion that is often associated with gene activation (Gross & Garrard, 1988; Grunstein, 1990; Svaren & Chalkley, 1991) may occur in part to enhance the deformability of the underlying nucleosomal array.

Quantitative Agarose Gel Electrophoresis as a New Tool for Studying Chromatin Structure and Function. Our results demonstrate that agarose gel electrophoresis can be used to determine several important physical properties of chromatin. The μ_o and surface electrical charge are determined quantitatively by the extrapolation of Ferguson plots to 0% agarose. The flexibility and deformability are determined qualitatively by measuring the effective R as a function of P_e. Each of these properties has been difficult to study with other techniques. In addition, differences in the shape of chromatin molecules can be detected at higher P_e (Figures 6 and 8; Table 1). In contrast to other quantitative biophysical techniques, gels require simple equipment and relatively small amounts of sample. By use of either radioactive or immunological probes, μ potentially can be measured for particles that are both impure and present in amounts as small as a nanogram. As a consequence, it should now be possible to use quantitative agarose gel electrophoresis to probe the structural features of specific, functionally interesting chromatin fragments isolated directly from cell nuclei.

ACKNOWLEDGMENT

We thank P. Schwarz and S. J. Hayes for excellent technical assistance, G. Griess for help with data analysis, and A. Wolffe for providing the bacterial strain that contained the pXP10 plasmid.

REFERENCES

Allen, M. J., Dong, X. F., O'Neill, T. E., Yau, P., Kowalczykowski, S. C., Gatewood, J., Balhorn, R., & Bradbury, E. M. (1993) *Biochemistry 32,* 8390–8396.

Bavykin, S. G., Usachenko, S. I., Zalensky, A. O., & Mirzabekov, A. O. (1990) *J. Mol. Biol. 212,* 495–511.

Borochov, N., Eisenberg, H., & Kam, Z. (1981) *Biopolymers 21,* 3089–3096.

Carr, K. D., & Richard-Foy, H. (1990) *Proc. Natl. Acad. Sci. U.S.A. 87,* 9300–9304.

Cullen, K. E., Kladde, M. P., & Seyfred, M. A. (1993) *Science 261,* 203–206.

Fangman, W. L. (1978) *Nucleic Acids Res. 5,* 653–665.

Fedor, M. J., Lue, N. F., & Kornberg, R. D. (1988) *J. Mol. Biol. 204,* 109–127.

Garcia-Ramirez, M., Dong, F., & Ausio, J. (1992) *J. Biol. Chem. 267,* 19587–19595.

Georgel, P., Demeler, B., Terpening, C., Paule, M. R., & van Holde, K. E. (1993) *J. Biol. Chem. 268,* 1947–1954.

Gottlieb, M. H., Steer, C. J., Steven, A. C., & Chrambach, A. (1985) *Anal. Biochem. 147,* 353–363.

Griess, G. A., Moreno, E. T., Easom, R., & Serwer, P. (1989) *Bioploymers 28,* 1475–1484.

Griess, G. A., Moreno, E. T., Herrmann, R., & Serwer, P. (1990) *Biopolymers 29,* 1277–1287.

Griess, G. A., Moreno, E. T., & Serwer, P. (1992) *Methods in Molecular Biology, Vol. 12: Pulsed-Field Gel Electrophoresis* (Burmeister, M., & Ulanovsky, L., Eds.) pp 173–181, Humana Press, Totowa, NJ.

Gross, D. S., & Garrard, W. T. (1988) *Annu. Rev. Biochem. 57,* 159–197.

Grunstein, M. (1990a) *Ann. Rev. Cell Biol. 6,* 643–678.

Grunstein, M. (1990b) *Trends Genet. 6,* 395–400.

Hansen, J. C., & Wolffe, A. P. (1992) *Biochemistry 31,* 7977–7988.

Hansen, J. C., & Lohr, D. (1993) *J. Biol. Chem. 268,* 5840–5848.

Hansen, J. C., Ausio, J., Stanik, V. H., & van Holde, K. E. (1989) *Biochemistry 28,* 9129–9136.

Li, R., Knight, J. D., Jackson, S. P., Tjian, R., & Botchan, M. R. (1991) *Cell 65,* 493–505.

Lohr, D., Torchia, T., & Hopper, J. (1987) *J. Biol. Chem. 262,* 15589–15597.

Lumpkin, O. J., DeJardin, P., & Zimm, B. H. (1985) *Biopolymers 24,* 1573–1593.

Mastrangelo, I. A., Courey, A. J., Wall, J. S., Jackson, S. P., & Hough, P. V. C. (1991) *Proc. Natl. Acad. Sci. U.S.A. 88,* 5670–5674.

McDonnell, M. W., Simon, M. N., & Studier, F. W. (1977) *J. Mol. Biol. 110,* 119–146.

Noolandi, J. (1992) *Advances in Electrophoresis* (Chrambach, A., Dunn, M. J., & Radola, B. J., Eds.) pp 1–56, VCH, Weinheim, FRG.

Olivera, B. M., Baine, P., & Davidson, N. (1964) *Biopolymers 2,* 245–257.

O'Neill, R. R., Mitchell, L. G., Merril, C. R., & Rasband, W. S. (1989) *Appl. Theor. Electrophor. 1,* 163–167.

Orbán, L., Garner, M. M., Wheeler, D., Teitz, D., & Chrambach, A. (1993) *Electrophoresis 14,* 720–724.

Pruss, D., & Wolffe, A. P. (1993) *Biochemistry 32,* 6810–6814.

Richard-Foy, H., & Hager, G. L. (1987) *EMBO J. 6,* 2321–2328.

Rodbard, D., & Chrambach, A. (1970) *Proc. Natl. Acad. Sci. U.S.A. 65,* 970–977.

Schmid, A., Fascer, K.-D., & Hörz, W. (1992) *Cell 71,* 853–864.

Serwer, P. (1980) *Biochemistry 19,* 3001–3004

Serwer, P. (1983) *Electrophoresis 4,* 375–382.

Serwer, P. (1986) *Methods Enzymol. 130,* 116–132.

Serwer, P., & Hayes, S. J. (1982) *Electrophoresis 3,* 80–85

Serwer, P., & Allen, J. L. (1984) *Biochemistry 23,* 922–927.

Serwer, P., & Dunn, F. J. (1990) *Methods (San Diego) 1,* 142–150.

Serwer, P., Allen, J. L., & Hayes, S. J. (1983a) *Electrophoresis 4,* 232–236.

Serwer, P., Watson, R. H., Hayes, S. J., & Allen, J. L. (1983b) *J. Mol. Biol. 170,* 447–469.

Seyfred, M. A., & Gorski, J. (1990) *Mol. Endocrinol. 4,* 1226–1234.

Shaw, O. J. (1969) *Electrophroresis,* Academic Press, London.

Simpson, R. T., Thoma, F., & Brubaker, J. M. (1985) *Cell 42,* 799–808.

Slater, G. W., Rousseau, J., & Noolandi, J. (1987) *Biopolymers 26,* 863–872.

Slater, G. W., Rousseau, J., Noolandi, J., Turmel, C., & Lalande, M. (1988) *Biopolymers 27,* 509–524.

Stellwagen, N. (1985) *Biopolymers 24,* 2243–2255.

Stellwagen, N. (1987) *Advances in Electrophoresis* (Chrambach, A., Dunn M. J., & Radola, B. J., Eds.) pp 179–208, VCH, Weinheim, FRG.

Su, W., Jackson, S. P., Tjian, R., & Echols, H. (1991) *Genes Dev. 5,* 820–826.

Svaren, J., & Chalkley, R. (1991) *Trends Genet. 6,* 52–56.

van Holde, K. E. (1988) *Chromatin,* Springer-Verlag, New York.

van Holde, K. E., & Weischet, W. O. (1978) *Biopolymers 25,* 1981–1988.

Wolffe, A. P. (1992) *Chromatin, Structure and Function* Academic Press, New York.

Wolffe, A. P., Jordan, E., & Brown, D. D. (1986) *Cell 44,* 381–389.

Workman, J. L., & Buchman, A. R. (1993) *Trends Biochem. Sci. 18,* 90–95.

Yao, C., Lowary, J., & Widom, J. (1991) *Biochemistry 30,* 8408–8414.